SANDIA REPORT

SAND98–2668
Unlimited Release
Reprinted December 1998

Parameter Optimization Applied to Use of Adaptive Blades on a Variable Speed Wind Turbine

G. Richard Eisler, Paul S. Veers

Prepared by
Sandia National Laboratories
Albuquerque, New Mexico 87185 and Livermore, California 94550
for the United States Department of Energy
under Contract DE-AC04-94AL85000

Issued by Sandia National Laboratories, operated for the United States Department of Energy by Sandia Corporation, a Lockheed Martin Company.

Printed in the United States of America. This report has been reproduced directly from the best available copy.

Available to DOE and DOE contractors from
Office of Scientific and Technical Information
PO Box 62
Oak Ridge, TN 37831

Prices available from (615) 576-8401, FTS 626-8401

Available to the public from
National Technical Information Service
US Department of Commerce
5285 Port Royal Rd
Springfield, VA 22161

NTIS price codes
Printed copy: A02
Microfiche copy: A01

SAND98-2668
Unlimited Release
Printed December 1998

Parameter Optimization Applied to Use of Adaptive Blades on a Variable Speed Wind Turbine

G. Richard Eisler
Advanced Engineering and Manufacturing Software

Paul S. Veers
Wind Energy Technology

Sandia National Laboratories
P.O. Box 5800
Albuquerque, NM 87185-1010

Abstract

The value of adding adaptive blades to a variable speed turbine is studied by applying a general purpose optimization scheme to a baseline turbine configuration. The turbine is the AWT-26. Adaptive-blade effects involve elastic twist coupling tied to centrifugal and flap loadings. Two baseline variable speed approaches are examined. In the "aggressive" approach the speed control is assumed to limit power output perfectly at the rated level, producing the theoretical maximum energy. In the "conservative" approach, speed control is not used at all to limit power; the power is limited by passive stall regulation. The adaptive blades do not substantially improve the performance of the aggressive, theoretical maximum. However, adaptive blades with centrifugal coupling are shown to make up 45% of the difference between the aggressive and conservative baseline cases when applied to the conservative speed control case. Simple pitch adjustments can also compensate for the conservative speed control in low wind sites, but in moderate to high wind sites the adaptive blades achieve substantially more. Cases including simultaneous centrifugal and flap coupling could not be studied with the optimization procedure because they amount to an over parameterization of the problem; i.e., there are many local maxima in the system performance criterion.

Summary

A parameter optimization study to improve average annual energy capture was conducted on a computational model of the two-bladed AWT-26 turbine. The thrusts of the study were to examine variable speed operation and adaptive blade measures. It is felt that present and future technology developments will make variable speed operation advantageous. Interest in adaptive blade measures has been fueled via recent studies that have shown marked improvements in system performance by coupling blade twist with rotor loads.

Optimization was applied as a "wrapper" around the industry-standard PROP performance analysis code. PROP models wind turbine operation as a quasi-steady process combining geometry, twist, and aerodynamic data to compute force, moment, and generated power as a function of tip speed ratio. The original code was modified to accept rpm's, local wind speed, and a blade pitch functional. Tip speed ratio was computed and power was extracted from PROP over a range of local wind speeds. These values were combined with a Rayleigh probability density function for a given average annual wind speed and integrated over local wind speed to compute an average annual power. The optimization problem was cast to maximize this average power metric for a given average annual wind speed while maintaining an upper limit on power over the local wind speeds. The Modified Method of Feasible Directions nonlinear programming technique was used to do the parameter optimization. The decision parameters were embedded in functionals for rotor speed and blade pitch. Blade pitch adaption models include dependencies on a constant offset, current rpm value, and a nominal bending moment value.

Two variable-speed operational modes were examined via optimization. The first was an "aggressive" mode allowing rpm's to vary at will as a function of local wind speed. The second was a "conservative" mode in which rpm's were allowed to increase with wind speed. In high winds, however, the speed is fixed at a speed that would allow stall regulation at a self-imposed 200-kilowatt power limit. Therefore, the speed increases linearly in low winds up to the speed at which the turbine will stall regulate at 200kW and then will operate at constant speed. Since this power limit is severe compared to the nominal turbine operation, the optimized conservative mode served as a baseline. Average power was maximized for 5,7, and 9 meters/sec average annual wind speeds while maintaining the upper power limit. The aggressive mode produced rotor speeds that were well over the nominal AWT-26 speed (57.1 rpm's) and a 7-10% increase in average power over average wind speed range versus the conservative mode. The final polynomial functional for blade pitch included a constant offset and a quadratic dependence on rpm's. Blade adaption was more effective in the conservative case, where rotor speed was constrained. An attempt to add bending-moment dependency into the blade pitch functional produced no gain, as it appeared to over-parameterize the problem.

Comparison of the variable-speed and adaptive-blade approaches to increase average power show that their effects are intertwined. If one is constrained, the other can compensate. In the aggressive speed case, rotor speed was essentially unconstrained and blade adaption had minimal effect.

Table of Contents

Table of Figures

Introduction

One of the basic requirements of wind turbine control is to ensure that the rotor does not produce more power than the rest of the system (drive train, generator, etc.) can withstand. The simplest approach is passive stall regulation that uses the characteristics of the airfoils to stall in high winds and regulate the power production of the rotor with no moving parts. More advanced controllers use changes to the rotor configuration to maximize system efficiency while the wind speed is fluctuating. Examples are variable speed, variable pitch (either full span or tip actuation), ailerons, passive pitch actuators and the like. There is a balance to be struck between the complexity of the control system, and hence the cost and maintainability of the system, and the ability of the controller to limit loads and/or to deliver more energy.

Enhancing stall regulation has long been a strategy for reducing wind turbine cost of energy. Increasing rotor size while holding the power rating constant allows all costs except the blades to remain relatively constant. At the same time an increase in net energy is obtained because the larger rotor captures more energy in low winds where efficiency is high and most of the annual energy is to be found. Tangler [1] uses this strategy to initially guide the development of the SERI family of airfoils, some of which stall at lower than usual angles of attack and therefore regulate at lower wind speed.

A previous study by Lobitz [2] showed how a substantial improvement in system performance can be realized by enhancing the stall regulation of a constant speed system via adaptive blade twist. The adaptive blade twists elastically in response to loads, creating a change in the angle of attack and thus influencing loads and power production. The approach described in the Lobitz paper assumes that the blade twists toward stall in response to loads that are proportional to either wind speed or power (e.g., flap loads) and therefore enhances power regulation. By increasing the rotor size while enhancing regulation using adaptive blades, a fixed power limit can be maintained while increasing net energy. Energy production grows in excess of the increase in rotor swept area with only modest elastic blade twist (2 degrees). While this result illustrates one specific application of the adaptive twisting blade to improve system performance, many significant issues need to be addressed before the adaptive blade can be proposed as a definite improvement. A more systematic evaluation of the benefits of the adaptive concept needs to be done in a variety of applications. This study looks at improvements in net energy production through systematic optimization of rotor operational parameters; future work will evaluate dynamic-load effects.

There is a strong sentiment in the US wind energy community that variable-speed systems will dominate the market in the near future, driven by cost reductions and improvements in power electronics. The value of adaptive blades needs to be evaluated in this variable-speed environment. The question remains whether elastic twist designed into a blade structure can add value to a variable speed system either by improving the theoretical maximum energy delivered in variable speed operation or by replacing an active control element with an inherently more robust passive element.

The Baseline Configuration

This optimization study uses the AWT-26 rotor as a baseline configuration from which to study adaptive blade enhancements. The airfoil selection and basic layout of the blade are therefore based on a pre-existing design and are not part of the optimization. Only the control features involving variable speed selections and elastic twist coefficients are included. The AWT-26 turbine (Figure 1) is rated at 300 kilowatts (kW) and is a two-bladed, downwind, teetered, free yaw, fixed pitch, stall controlled, constant speed, horizontal-axis wind turbine. The rotor is 26 meters (m) in diameter. The normal operating speed is 57 revolutions per minute (rpm's). For analysis purposes, a blade is divided into ten segments, which have associated twist and airfoil characteristics. Blade twist is displayed as a function of normalized chord (local chord length/blade length) in Figure A-1 in the Appendix. Lift and drag curves per segment as a function of angle of attack are shown in Figure A-2. Blade pitch is fixed at +1.2 degrees; positive implies pitch to feather, negative is pitch to stall.

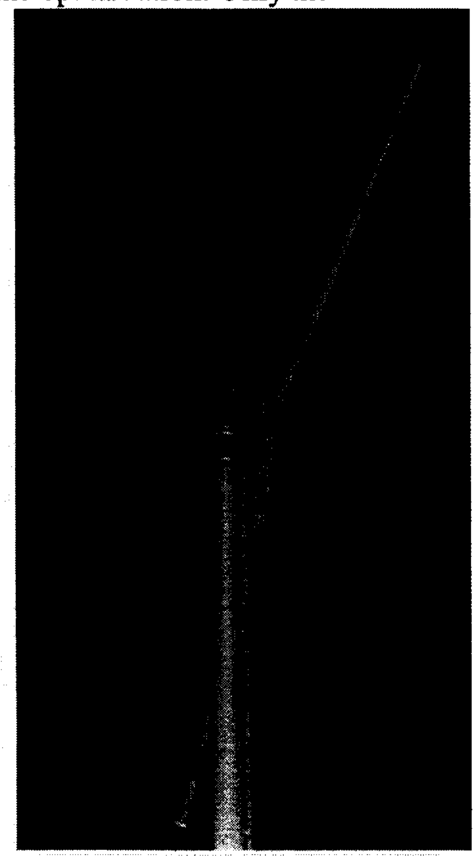

Figure 1. AWT-26 Turbine

Overview of the Study

The point of this study is to see if adaptive blades that enhance stall regulation can achieve substantial benefits in a fixed-pitch, variable-speed environment. Since the baseline turbine already regulates quite well in constant speed mode at 300kw, there is no additional gain to be had under those conditions. In the previous study [2] the power limit was held at 300kw while the rotor size was allowed to grow with improving ability to stall regulate. Here, rather than growing the rotor diameter, we reduce the target maximum power from 300kw to 200kw. This ensures that the power bound is violated for obtainable rotor speeds and that the optimization has to compensate.

A rotor designed to have a high efficiency at a particular tip speed ratio can theoretically be operated at that constant tip speed ratio below rated power to achieve the maximum energy capture. Power can theoretically be maintained at the rated level above the rated wind speed by lowering the speed to reduce the efficiency. (This is essentially what is done with variable pitch, where pitching the blade reduces the efficiency and keeps the rotor from overproducing. Here we focus on fixed pitch to see if the adaptive blades can supply a function similar to active pitch, but without the expense of the mechanism.) The term "theoretically" is used because, first, the turbine can never be operated exactly at the target tip speed ratio because of the transient nature of the wind, and, second, it may not be possible to maintain a constant power using speed control alone without substantially oversizing the generator and drive train. The first issue is one for which adaptive blades might have application, but requires dynamic analysis to evaluate and will not be dealt with here. The second issue is the primary focus. It will be shown that the speed variations necessary to limit power output using speed control alone are extreme. In addition, the generator must extract energy from the kinetic energy of the rotor to slow it down, and do it exactly when the generator is already at rated power [3],[4]. Such speed variations may not be possible to implement without substantially oversizing the generator and drive train to allow "headroom" for overshooting the rated power.

This study examines the ability of adaptive blades to regain some of the theoretical advantage of variable speed, but with a conservative and easily implemented control strategy. Two different variable speed scenarios are therefore examined. The first, or *aggressive* approach, allows rotor speed to assume arbitrary values as a function of wind speed. This gives maximum variable speed control without regard for whether it is achievable or not. It produces a theoretical maximum against which other results can be compared. The second, or *conservative* approach, allows rotor speed to increase until it reaches a point where the rotor will stall regulate at 200kw at that speed. The rotor speed is fixed at this value in high winds. This provides a lower bound for what variable speed alone can achieve. Adaptive blade effects are applied to both scenarios to see how they can affect the theoretical maximum (in the aggressive approach) and if they can regain some of the lost energy sacrificed in conservatively operating a variable-speed turbine. If sufficient energy can be regained in the conservative approach, it may be possible to operate a variable speed rotor with stall regulation and without excessive headroom.

Analysis

A gradient-based parameter optimization method is used to query the quasi-steady PROP wind turbine performance analysis code [5]. The decision parameters describe rotor speed variation with wind speed and blade pitch dependencies on current rpm and bending moment. Rotor configuration and airfoil data, shown in the Appendix, are used as input to the PROP analysis code. PROP uses momentum-strip theory to calculate loads and performance. This is a quasi-steady analysis and as such does not include transient dynamics. PROP was modified from its original configuration of computing over a range of tip speed ratios (TSR's) to computing thrust, moments, and power at a single TSR. An outer loop was wrapped around PROP to compute a TSR from a designated rpm and wind speed (where the TSR is $R\Omega/V$, for rotor radius R rotor rotation speed Ω and wind speed V). Inside PROP, blade pitch adjustments were simply added to the nominal +1.2 degree value. By varying V and Ω for a given blade pitch, a dependent variable "response" grid can be generated. Two dependent variable responses, for power and blade-root bending moment, are shown below.

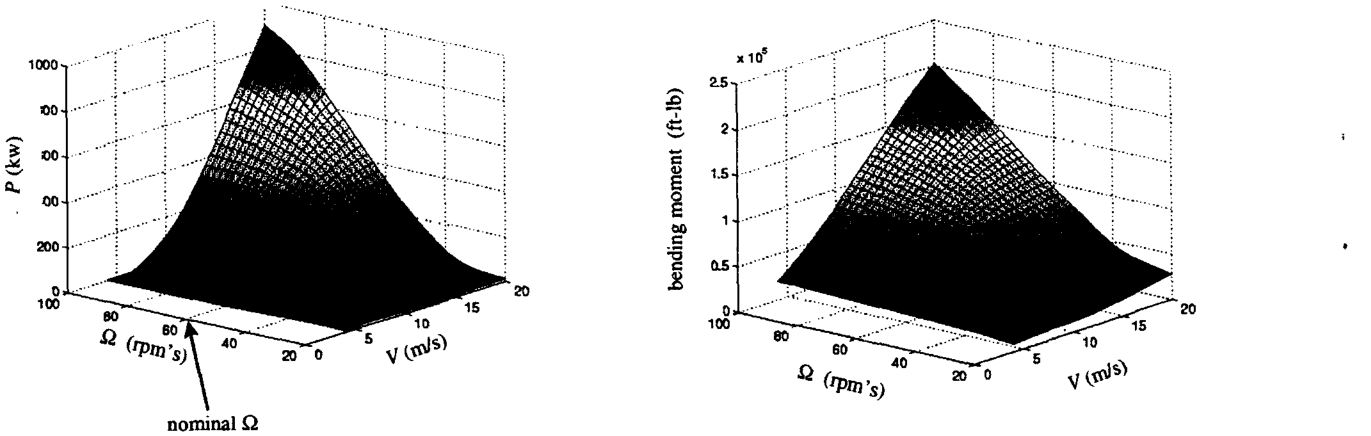

Figure 2. PROP output for AWT-26 model

As energy optimization was the goal of the study, a metric proportional to average annual energy was chosen. By using the power, *P*, computed in PROP, and combining it with a wind speed probability distribution function, the result can be integrated over wind speed to produce an average annual power. This metric is proportional to average annual energy. A Rayleigh probability distribution that is characterized by an average wind speed at a site is given by

$$f(V) = \frac{2}{\overline{V}} * \frac{\pi}{4}\left(\frac{V}{\overline{V}}\right)^2 \exp\left[-\frac{\pi}{4}\left(\frac{V}{\overline{V}}\right)^2\right], \quad [1]$$

where V is instantaneous wind speed and $\overline{V}$ is the annual average wind speed. The average annual power is then given by

$$\overline{P}(\overline{V}) = \int_{V_{\min}}^{V_{\max}} P(V) f(V) dV . \quad [2]$$

The power output from PROP is shown in Figure 2 and the transformation to the integrand value, $P(V)f(V)$, is shown in Figure 3 for $\overline{V} = 5$ meters/sec (m/s). Average wind speeds of 5, 7, and 9 m/s are examined in this study. Note that the result of transforming the power via the Rayleigh distribution accentuates performance in the lower wind speeds and lessens in importance of generation at higher speeds. Therefore, if more power could be generated at the lower wind speeds via variable rotor speed or adaptive blade measures, then $\overline{P}$ will increase. This is the goal of the optimization efforts.

If only rotor speed as a function of wind speed is of interest, the grid shown in Figure 3 could be sequentially searched for rotor speed values that would maximize $P(V)f(V)$, as well as maintain power between specified bounds. Since $P(V)f(V)$ is always positive, maximizing its magnitude will also maximize the integral, $\overline{P}(\overline{V})$.

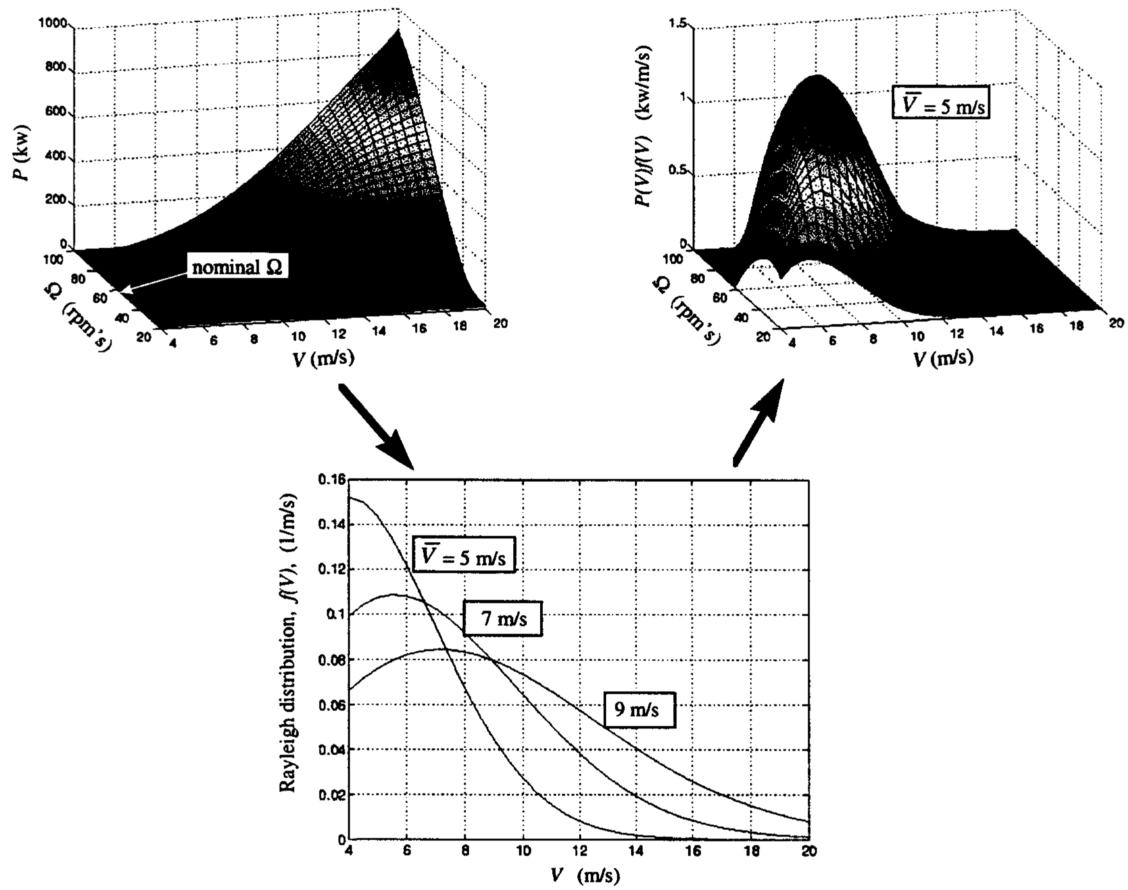

Figure 3. Power to Average Power Conversion

Search results are shown in Figure 4, where the maximum values of $P(V)f(V)$ are shown as a solid line superimposed on the surface in three dimensions. An upper power bound for this search was chosen to be 200 kW, as explained above. The projection of the $[P(V)f(V)]_{max}$ curve onto the *wind speed-rpm* plane gives the "control" history that maximizes $\overline{P}(\overline{V})$. The projection of the $[P(V)f(V)]_{max}$ curve onto the $P(V)f(V)$ - *wind speed* plane gives the curve whose integral is the annual power performance metric, $\overline{P}(\overline{V})$.

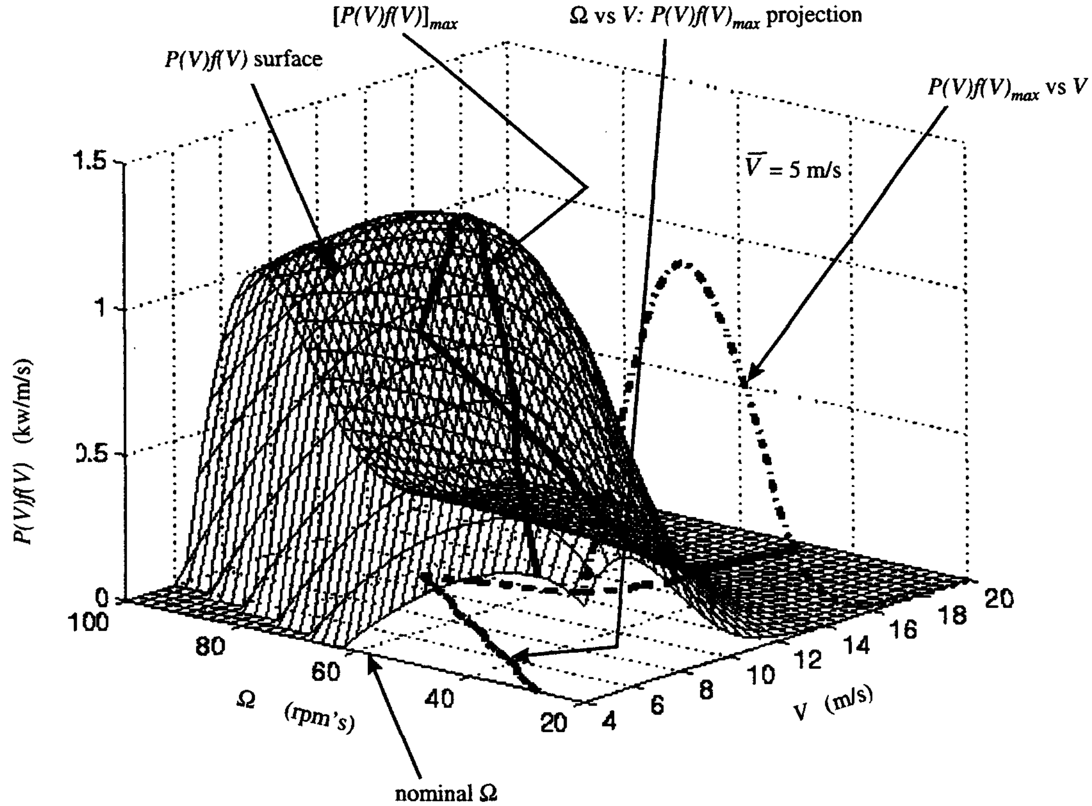

Figure 4. Average Power Grid Components

Recall that to test the efficacy of an optimization technique in tuning speed and blade pitch, the power limit of the nominally 300kw turbine was reduced to 200kW for this study. This would insure that the power bound would be violated for obtainable rotor speeds and that the optimization method would have to compensate. Two different rotor speed scenarios were parameterized and compared to maximize $\overline{P}(\overline{V})$, while maintaining the upper power bound. The first, or *aggressive* approach, allowed rotor speed to assume arbitrary values as a function of wind speed. This required a rotor speed parameter value, $\Omega_i(V_i)$, at each value of wind speed (Figure 5). Wind speeds covering the range from 4 to 20 m/s in 0.5 m/s increments were selected to provide an accurate numerical computation of the integral $\overline{P}(\overline{V})$. Note that small variations in Ω at the higher wind speeds can cause abrupt variations in power. The second, or *conservative* approach, allowed rotor speed to linearly increase as a function of wind speed until it reached a point that the first violation of the power bound occurred at *any* wind speed. After this point, the rotor speed remained fixed at this value. This approach required only 3 parameters, an initial rotor rpm value (Ω_0), a constant slope, and a final rpm value (Ω_{max}) as shown in Figure 5. Ω_0 is assumed to be at 4 m/s and the slope places Ω_{max} at the desired wind speed.

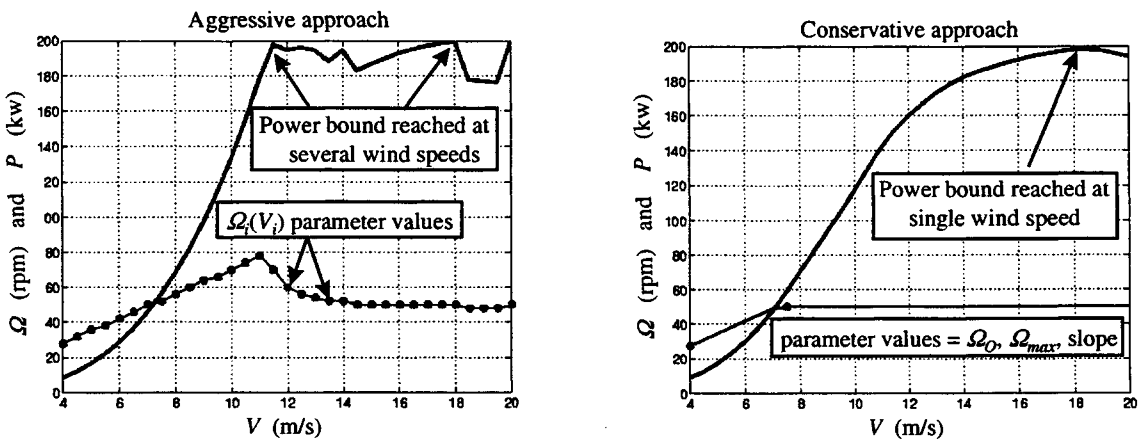

Figure 5. Rotor Speed Parameterization Approaches

As stated previously, the AWT-26 turbine has blades pitched 1.2 degrees to feather, nominally. To assess possibilities for adaptive blade operation, a polynomial combining the effects of a constant angle offset, rotor speed, and bending moment was used to change the effective pitch angle across the range of local wind speeds. The effective pitch angle at a given wind speed, V_i, was

$$\theta_{effective}(V_i) = 1.2 + k_0 + k_1\left(\Omega(V_i)/60\right)^2 + k_2\left(BendingMoment(V_i)/10^5\right) \qquad [3]$$

where k_0 is a constant offset angle and k_1, k_2 are multiplicative constants. These *parameters* are added to those of the chosen speed control approaches described previously to complete a given parameter set for optimization. Ω and bending moment have been normalized to keep values in the zero to one range. The bending moment history was obtained from an optimization history where only Ω was optimized. Therefore, there is no iteration on bending moment; the bending moment without pitching is used to determine the change in pitch due to the bending-twist coupling. Note that the rotor speed effect on $\theta_{effective}$ is quadratic to model the speed-driven centrifugal force coupling.

The major problem with the model from a numerical standpoint is its use of a nonlinear numerical solution as a prelude to computing forces and moments. One of the avenues of exploration in this study is to search out appropriate Ω's over a range of wind speeds to maximize $\overline{P}(\overline{V})$. As seen in Figure 3, increasing P at the lower wind speeds is critical to this goal. Figure 6 shows an example of PROP power computation for varying rotor speed for a fixed local wind speed of 6 m/s and the nominal 1.2 degree blade pitch angle. On the macro-scale of 40 - 60 rpm, the power appears to smoothly decrease. However, on examining a micro-region of the curve, this decrease is really an average behavior of a noisy output. The problem is that noise wreaks havoc with gradient-based numerical optimization techniques. Attempts to use analytic gradient solvers [6] to generate the partial derivatives, $\frac{\partial P_i}{\partial \Omega_i(V_i)}, \frac{\partial P_i}{\partial k_j}$ failed because of the noise severity; finite-difference gradient approximations were used instead. Measures taken to alleviate (but not eradicate) this problem included the use of higher solution tolerances for the nonlinear solver, converting PROP to double precision, and the use of larger parameter variations, $\Delta\Omega_i(V_i), \Delta k_j$, in the finite-difference computation of the partial derivatives.

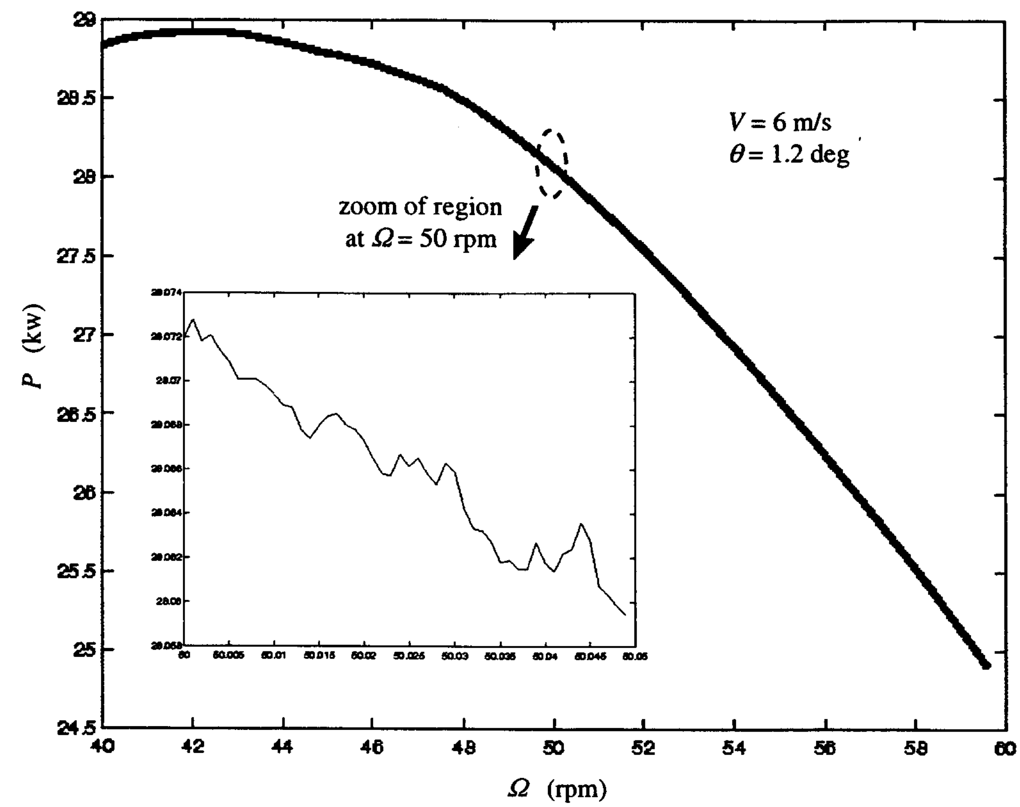

Figure 6. Coarse- and fine-scale PROP output

Optimization Methodology

The optimization method used was the Modified Method of Feasible Directions (MMFD) written by G. Vanderplaats [7] and provided as an option in the DAKOTA optimization environment developed at Sandia National Laboratories [8]. The MMFD method attempts to minimize a scalar performance metric, $F(\vec{\xi})$, which is a function of parameter vector $\vec{\xi}$, subject to a vector of constraints, $\vec{C}(\vec{\xi}) \leq 0$. Since we are seeking to maximize average power (in this minimization environment) and there is only a single active constraint, the problem specifications are

$$\textit{minimize}: -\overline{P}(\overline{V}) \text{ subject to } P(V,\vec{\xi}) \leq 200\,\text{kW for } 4 \leq V \leq 20\,\text{m/s}, \vec{\xi} = \left[\Omega_i(V_i), k_0, k_1, k_2\right] \quad [4]$$

Power is being sampled from PROP at discrete values of local wind speed, V_i, in order to compile approximations to the performance metric and constraint dissatisfaction. To accommodate this sampling, the actual metric and constraint are posed as follows:

$$\textit{Performance Index}: F(\vec{\xi}) = -\overline{P}(\overline{V}) \approx \Delta V \sum_{i=1}^{N} P_i(V_i,\vec{\xi}) f(V_i,\overline{V})$$

$$\textit{Constraint Dissatisfaction}: \vec{C}(\vec{\xi}) \approx \sum_{i=1}^{N} \max\left[P_i(V_i,\vec{\xi}) - 200., 0.\right], \quad [5]$$

where N=33 velocities sampled at ΔV=0.5 m/s increments over the 4-20 m/s range. Note that the individual terms in the constraint dissatisfaction summation will either produce a positive quantity if $P_i(V_i\vec{\xi}) > 200$ or zero if it is less. Since the MMFD method expects satisfied constraints to be of the form, $\vec{C}(\vec{\xi}) \leq 0$, the use of the above approximate form will show satisfaction when $\vec{C}(\vec{\xi}) = 0$. (i.e., the output from PROP, $P_i(V_i,\vec{\xi})$, never exceeds 200 kW). Since only a single constraint exists in this study, the vector arrow over the C will be henceforth omitted.

$F(\vec{\xi})$ and $C(\vec{\xi})$ were of the same form as above for all computations; only the composition of $\vec{\xi}$ changed, as well as the average annual wind speed, $\overline{V}$.

Results

As stated previously, two different rotor speed scenarios, aggressive and conservative, were optimized as shown in Figure 5. For both, the following adaptive blade measures were also simultaneously applied:

[Case 1] $\theta_{effective}(V_i) = 1.2$ degrees (nominal blade pitch, no optimization)

[Case 2] $\theta_{effective}(V_i) = 1.2 + k_0$

[Case 3] $\theta_{effective}(V_i) = 1.2 + k_0 + k_1(\Omega(V_i)/60)^2$

[Case 4] $\theta_{effective}(V_i) = 1.2 + k_0 + k_1(\Omega(V_i)/60)^2 + k_2(\text{Bending Moment}(V_i)/10^5)$

Results were generated for annual wind speeds, $\overline{V} = 5, 7,$ and 9 m/s.

Figure 7 shows results for the baseline optimization of the rotor speed history only for nominal blade pitch (item 1 in the above list). The baseline conservative optimization has only three parameters (Ω_{min}, Ω_{max}, *slope*) that need to be adjusted. The Ω histories rise linearly from 27 rpm to a maximum value of 50 rpm at about 7 m/s.

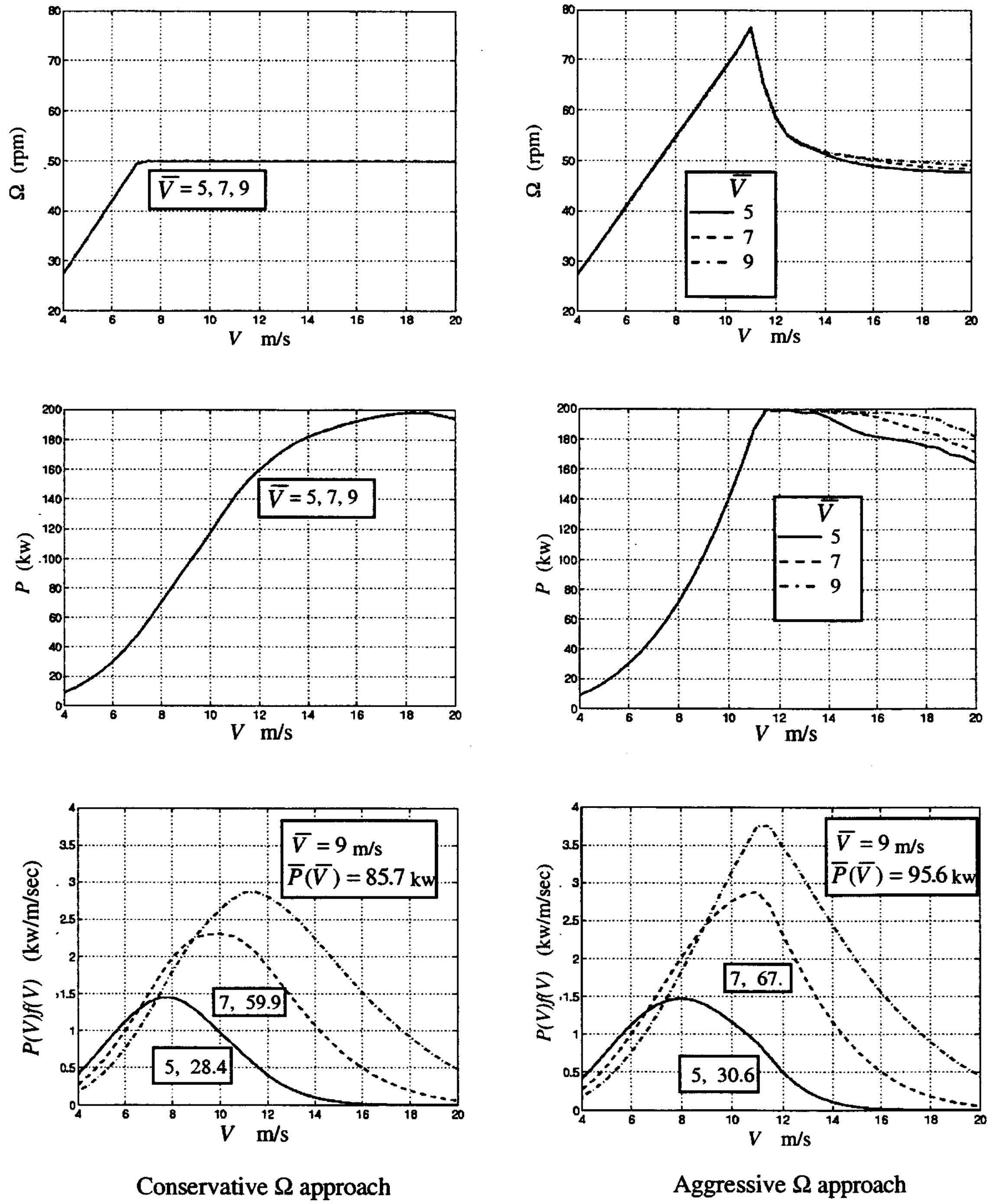

Figure 7. Rotor Speed Optimization Results for Nominal Blade Pitch
[Case 1]

The Ω histories for this approach are identical because the outcome is only contingent on the lowest Ω value encounter with the 200kW power bound, which occurs at 18 m/s and is not a function of $\overline{V}$. There is no chance of increasing P at lower wind speeds, because of this encounter. Note that the Rayleigh weighted power, *P(V)f(V)*, suffers less high-speed decay and increases in overall value as $\overline{V}$ increases.

The baseline aggressive-approach results in Figure 7 show a near linear rise in Ω with wind speed from 27 rpm to 76 rpm, and then falls off precipitously to ensure that the 200kW power bound is not violated. The optimization has, therefore, found a region in the moderate wind speeds where power can be increased via a peak in Ω to affect the annual power integral, $\overline{P}(\overline{V})$. Note that the aggressive approach is able consistently to maintain power near the bound if there is significant energy to be gained. The optimization pushes the power closer to the 200kW barrier in high winds as those winds become more important. In the 5 m/s case, for example, power output above 15 m/s is virtually irrelevant. $\overline{P}(\overline{V})$ differences, (aggressive-conservative)/conservative, range from 7-12% for $\overline{V}$ = 5-9 m/s.

Figure 8 shows these comparisons for a constant offset (or bias) in the pitch angle, where $\theta_{effective} = 1.2 + k_0$ (k_0 being the optimized offset in degrees). In all cases the tendency was to reduce the blade angle, which was originally pitched to feather. The reduction was on the order of one degree. The conservative Ω histories are again identical, due to the "1st bound contact" at 18 m/s wind speed. However the rpm value to achieve this is now slightly higher at 52 rpm versus the nominal pitch case and occurs at a higher wind speed. The energy metric, $\overline{P}(\overline{V})$, shows a 3.0-3.6% increase across the span of $\overline{V}$ versus the nominal-pitch, conservative-Ω case.

The aggressive-approach results have changed in this case to display nearly identical rotor speed histories characterized by the familiar linear increase at the low and moderate wind speeds, followed by a rotor speed drop-off to satisfy the power bound. Ω at the higher wind speeds is asymptotic to the 52 rpm value found in the conservative approach. *P* more closely "hugs" the bound for all $\overline{V}$'s versus the nominal pitch case. $\overline{P}(\overline{V})$ shows only a 1-2% increase versus the nominal-pitch, aggressive-Ω case. Because the conservative approach benefits more from a readjustment of the pitch offset, the advantage of the aggressive speed control has dropped to 4-8%, with the least advantage still in the 5 m/s average winds.

Figure 9 shows the results of adding an Ω^2 dependency into the blade pitch equation. This term reflects an adaptive blade that twists in response to centrifugal loads. Use of this term produced many local $\overline{P}(\overline{V})$ maxima [as a function of $\Omega_i(V_i), k_0, k_1$] of nearly the same value, depending on the initialization of the k_0, k_1 constants. This signifies that a "flat" region in the parameter space has been reached. In this region, sensitivity to some part of the parameter set has been lost. The optimization algorithm is forced to generate an answer with insensitive parameters and has minimal good derivative information to change parameter values from the initial "guesses." This behavior was more evident for the aggressive approach.

The conservative approach with Ω^2 blade dependency increases rpm linearly with wind speed to a value greater than the constant-offset blade-angle case. The changeover from variable to constant speed also occurs at a higher wind speed, about 8 m/s. A spread of several rpm exists between the $\overline{V}$ =5 m/s case and the 7 and 9 m/s cases. Power curves are still roughly the same. $\overline{P}(\overline{V})$ values show about a 2% difference versus the constant offset case. A comparison of θ histories is shown in Figure 10. For all $\overline{V}$'s the tendency is to pitch the blade to stall for the 4-20 m/s local wind speed range. A $\Delta\theta$ difference of 1.0 degree exists between the 5 m/s and the 7 and 9 m/s curves, where the higher $\overline{V}$ histories are pitched further into the stall region.

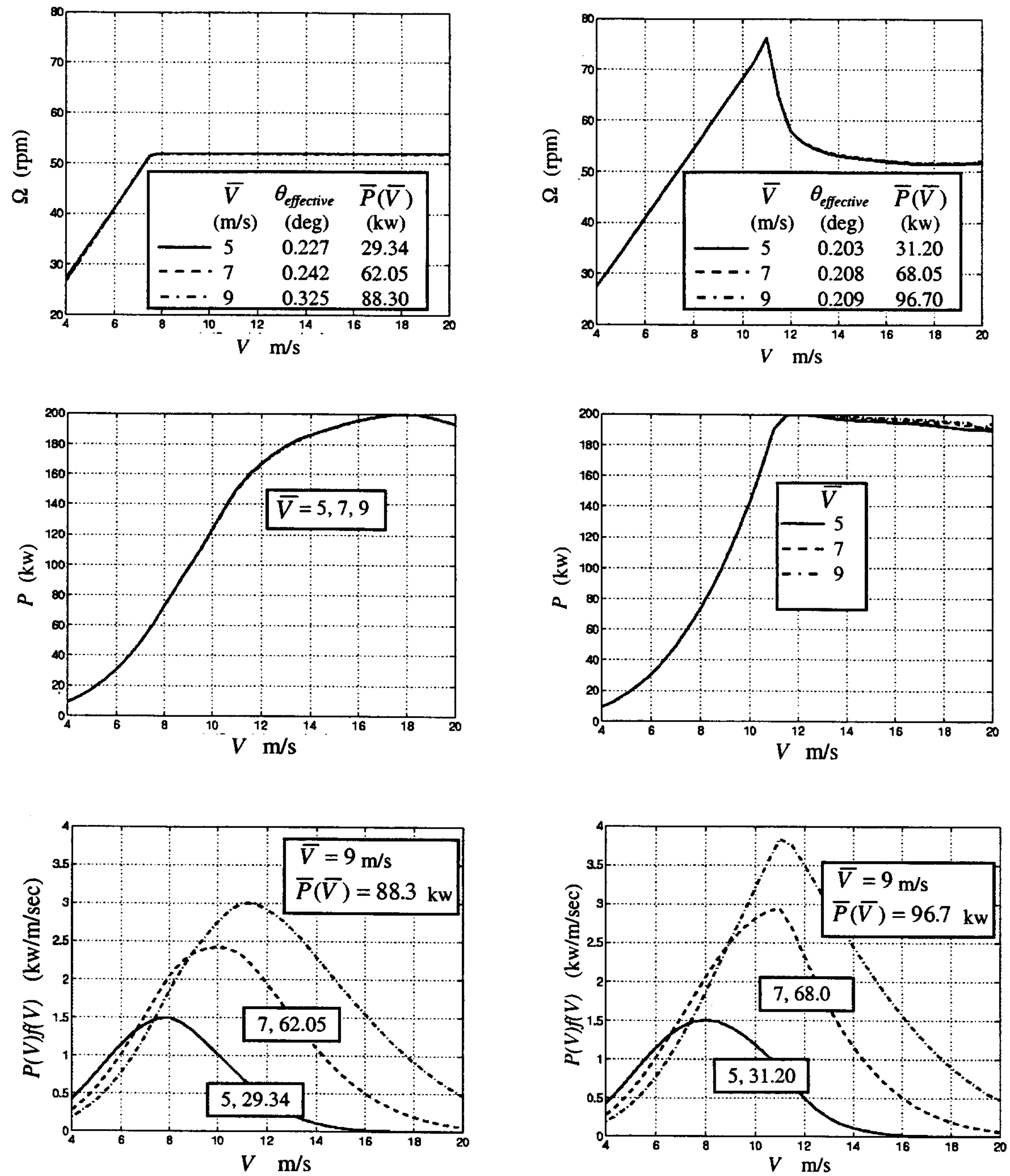

Conservative Ω approach

Aggressive Ω approach

Figure 8. Rotor Speed Optimization Results for Constant Offset Blade Pitch [Case 2]

The aggressive Ω approach with Ω^2 blade dependency displays almost no change from the constant offset case. Ω histories for all $\overline{V}$'s are essentially identical, which in turn show the same small power differences at the higher wind speeds. The blade histories in

Figure 10 demonstrate the *insensitivity* of the $\overline{P}(\overline{V})$ values with respect to this added adaptive blade feature. The optimization turned off the Ω^2 dependency at $\overline{V}$ =5 and 7 m/s leaving the blade with the constant offsets found previously. Clearly these are cases of over-parameterization or of the use of multiple terms in the modeling that have similar effects.

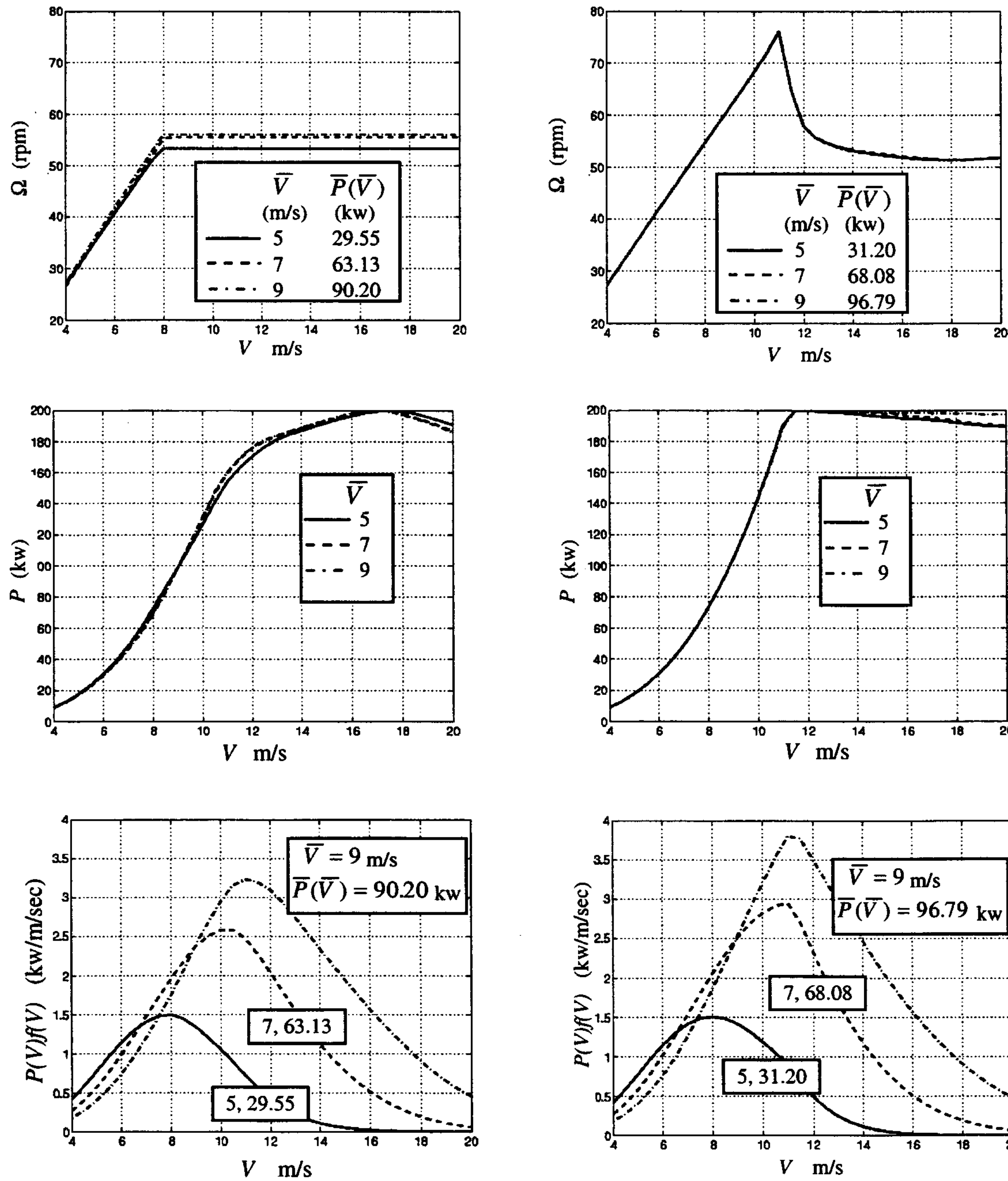

Conservative Ω approach | Aggressive Ω approach

Figure 9. Rotor Speed Approaches with Offset + Ω^2 blade pitch dependencies [Case 3]

At $\bar{V} = 9$ m/s the optimization activates the Ω^2 blade angle dependence, creating a θ history that looks very much like the Ω curve. However, the effect on $\bar{P}(\bar{V})$ is negligible. Obviously, another local maximum has been found with no advantage over the constant offset case.

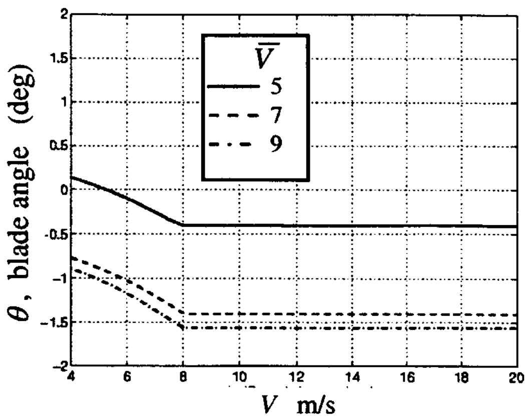

Conservative Ω Approach

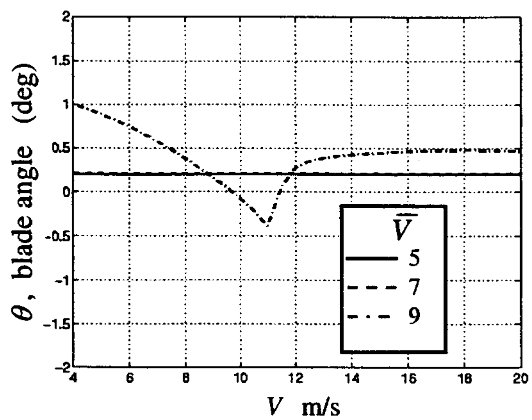

Aggressive Ω Approach

Figure 10. Adaptive Blade Angle Histories for Offset + Ω^2 Dependencies [Case 3]

A comparison with the conservative *offset* + Ω^2 approach was made by replacing the Ω^2 dependency with a linear dependence on nominal bending moment to assess any advantage. The $\bar{P}(\bar{V})$ results for the latter idea compared with those in Figure 9 are shown in the following table.

$\bar{V}$ (m/s)	$\bar{P}(\bar{V})$ (kW) $\theta = k_0 + k_1\Omega^2$	$\bar{P}(\bar{V})$ (kW) $\theta = k_0 + k_1 BM$
5	29.55	29.69
7	63.13	63.31
9	90.20	90.29

The change to bending moment (BM) shows only a slight improvement (< 1%) across the $\bar{V}$ range and with the inherent noise in the model is deemed to have an equivalent, but not superior effect to that of rotational speed.

Attempts were made to include the bending moment dependency (k_2) into the θ formulation as a third term (together with the *offset* and Ω^2 terms **[Case 4]**). This produced a variety of local maxima in both variable-Ω approaches, which demonstrated *no* advantage over less involved blade adaptations. The results were not plotted. These maxima entailed tradeoffs in value between the k_0, k_1, k_2 parameters much like the $\overline{V}$ =9m/s blade history shown previously in Figure 10. This scenario is an example of *over-parameterization,* where the modeled behavior can be successfully captured with fewer parameters and dependencies.

Figure 11 displays previously shown parameterizations isolated for $\overline{V}$ = 7 m/s and both Ω approaches. As seen before, rpm's at higher wind speeds increase if the blade is pitched from its nominal 1.2 degree setting toward stall. With the conservative Ω approach, there is more chance to affect the $\overline{P}(\overline{V})$ performance measure via blade adaptation versus the aggressive approach. This comparison demonstrates that variable speed and adaptive blade measures for annual power increase are intertwined and that one can compensate for constraints on or lack of the other. In the conservative variable speed approach, speed is moderately-to-severely constrained and blade adaptation has an impact [5% in $\overline{P}(\overline{V})$ values]. In the aggressive case, no constraints (other than maximum power) are put on rotor speed and the impact of blade adaptation is minimal (1%).

Figure 12 illustrates how simple pitch offsets and an adaptive blade with centrifugal-twist coupling are able to compensate for a conservative approach to variable speed control. A simple pitch change can recover a great deal of the theoretical losses of conservative speed control. In a low wind site (5 m/s) it may be sufficient, additional improvements are marginal. In higher wind sites, the adaptive blade can capture 45% of the difference between the baseline conservative and aggressive (theoretical maximum) cases.

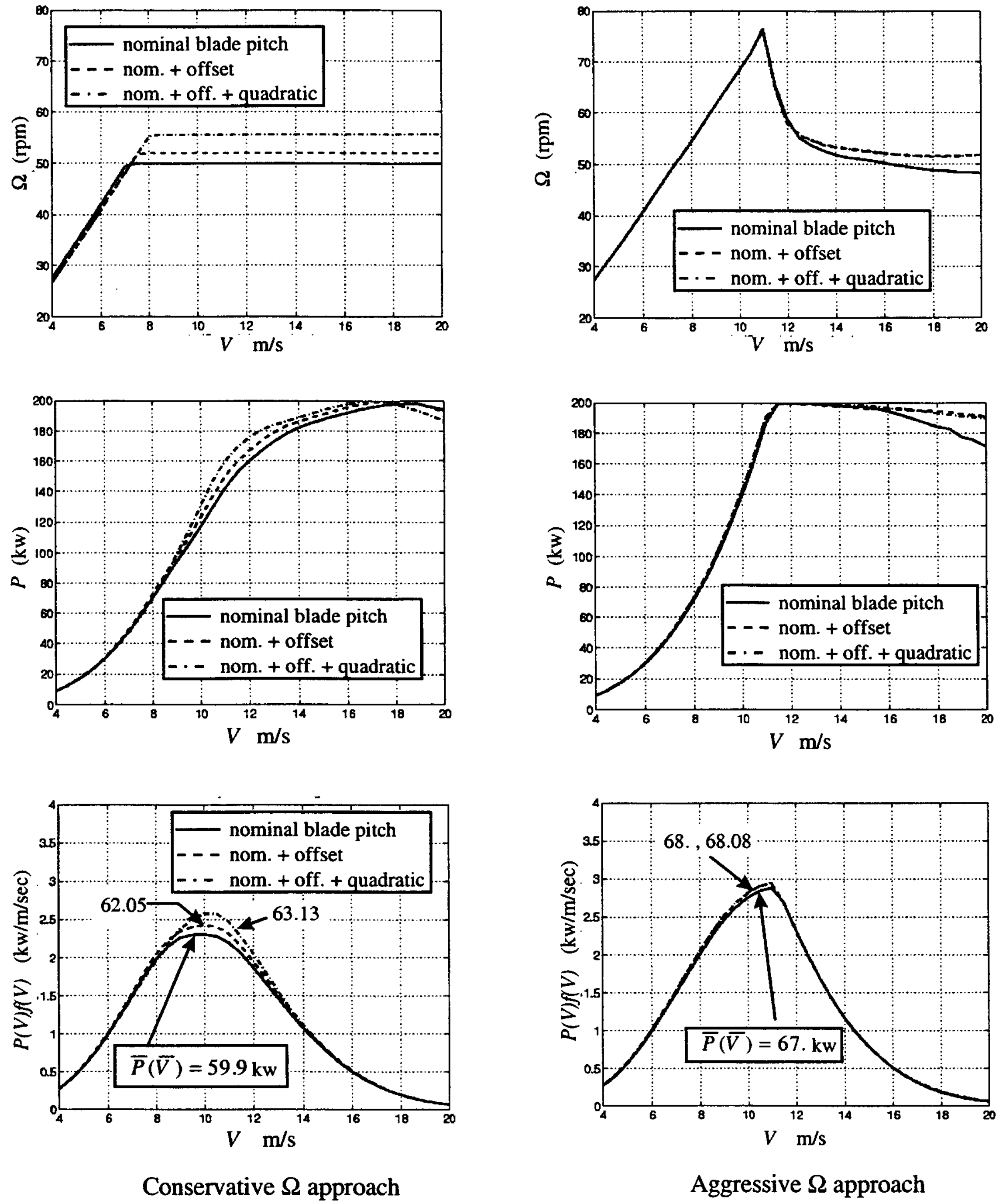

Figure 11. Comparison of Variable Speed / Adaptive Blade Schemes (for $\overline{V} = 7$ m/s)

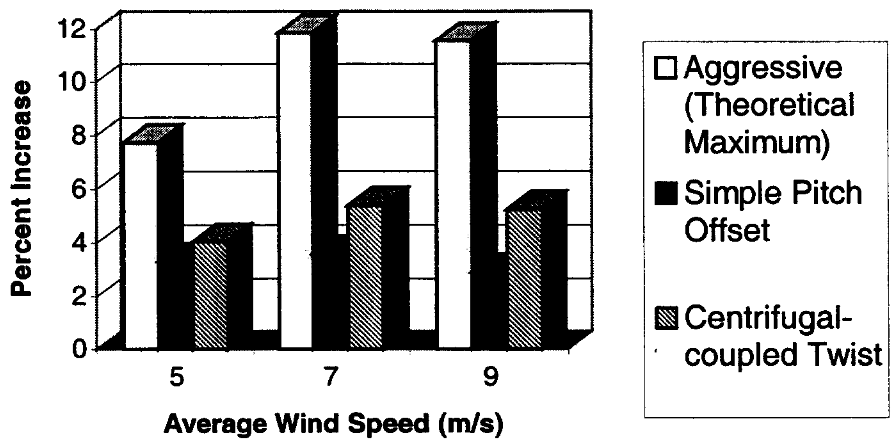

Figure 12. Average power increase above baseline conservative speed control case. ("Aggressive" allows any rotor speed at each wind speed; the other two cases are with the conservative speed control enhanced as stated).

Conclusions

This study sought to increase simulated average annual power for the AWT-26 turbine via the combination of variable speed and adaptive blade pitch measures. Gradient-based, numerical optimization was used to solve for parameters in function models for these two types of effects. The variable speed models were composed of 1) a conservative approach characterized by a linear rotor speed rise with local wind speed to a constant rpm; and 2) an aggressive model that had no behavioral constraints on speed other than to maintain an upper bound on power. Blade pitch models were summation combinations of the nominal blade setting, constant offsets, quadratic-in-rotor-speed dependency, and bending-moment dependency. The optimization problem consisted of maximizing average annual power while maintaining an upper bound on the power curve.

Average power is increased by operating at speeds that maintain maximum efficiency below rated power and are arbitrarily adjusted to regulate power above rating. This aggressive speed-control approach represents an upper bound on performance, although it may not be realizable due to the extreme changes in rotor speed required as a function of wind speed. This aggressive approach cannot be improved substantially by adaptive blade schemes. The greatest improvement was about 1%.

The conservative speed-control approach produces an average power 7-12% lower than the theoretical maximum. However, most of the losses resulting from the more workable speed control can be regained with some simple adaptations. A simple resetting of the pitch toward stall recovers about 3% of the total average power in all wind speed cases. This is 25% to 45% of the total difference between conservative and aggressive approaches. Relating the blade pitch changes to the square of rotor speed (centrifugal coupling) results in average powers 4% to 5.5% higher than the conservative case, a 45% to 52% recovery of the difference between conservative and aggressive approaches. The greatest improvement due to adaptive blade coupling is in the higher (7 and 9 m/s) average wind speeds. Results for a simple pitch change and an adaptive blade are about the same in the 5 m/s case. The improvements stem from an increase in maximum rotor speed and an increase in the wind speed at which the rotor switches to constant-speed operation, resulting in a greater range of operation at peak efficiency and higher efficiencies in the middle of the wind-speed operating range. The power curve is therefore boosted where the greatest annual energy is available in the higher wind cases.

It appears that adaptive pitch changes can compensate for constrained rotor speed operation in the regimes covered in this study to improve average annual power output. Where rotor speed is unconstrained, as in the aggressive approach, blade pitch compensation showed no ability to improve average power output.

References

[1] Tangler, J., "Atmospheric Performance of the SERI Thin Airfoil Family: Final Report," Proc. *Windpower '90,* American Wind Energy Association, Washington DC, Sept. 24-28, 1990.

[2] Lobitz, D. W. and P. S. Veers, "Enhanced Performance of HAWT's Using Adaptive Blades," Proc. *Energy Week '96, Book VIII Wind Energy,* (ASME Wind Energy Symposium) Houston, Texas, Jan. 29-Feb. 2, 1996.

[3] Muljadi, E., C. P. Butterfield, and P. Migliore, "Variable Speed Operation of Generators with Rotor-Speed Feedback in Wind Power Applications," Proc. *Energy Week '96, Book VIII Wind Energy,* (ASME Wind Energy Symposium) Houston, Texas, Jan. 29-Feb. 2, 1996.

[4] Muljadi, E., C. P. Butterfield, and M. L. Buhl, "Effects of Turbulence on Power Generation for Variable-Speed Wind Turbines," Proc. *1997 ASME Wind Energy Symposium,* AIAA-97-0963, held at the 35th AIAA Aerospace Sciences Meeting and Exhibit, Reno, Nevada, January 6-9,1997.

[5] Tangler, J., "A Horizontal Axis Wind Turbine Performance Prediction Code for Personal Computers," Solar Energy Research Institute, 1987, Golden, CO.

[6] Bischof, C. et al., " ADIFOR 2.0 User's Guide," Mathematics and Computer Science Division, Technical Memorandum No. 192, Argonne National Laboratory, Argonne, IL, August 1995.

[7] Vanderplaats Research and Development Inc., 1995 DOT Users Manual, Version 4.20, Colorado Springs, CO.

[8] Eldred, M.S. et al, "Utilizing Object-Oriented Design to Build Advanced Optimization Strategies with Generic Implementation," paper AIAA-96-4164 in *Proceedings of the 6th AIAA/USAF/NASA/ISSMO Symposium on Multi-Disciplinary Optimization,* Bellevue, WA, Sept 4-6, 1996, pp. 1568-1582.

Appendix A: AWT-26 Blade Aerodynamic and Twist Data

Tables of lift, drag, and twist data for the AWT-26 blades are used by the PROP code to compute performance. The AWT-26 rotor blades are 43 ft in length. Each is modeled as composed of 20 segments ordered from hub to blade tip. Twist data as a function of normalized blade chord is shown in Figure A- 1. The segments 1 (closest to hub) and segment 2 have identical twist values. Segment 7 has the largest blade chord. Blade segment lift and drag data as a function of angle of attack are shown in Figure A- 2. Aerodynamic data is approximated as duplicated for every two adjacent segments from hub to tip for a total of 10 individual curves. Note that the lift data is highly variable and is a maximum where blade chord is the largest. Drag data displays small variations from one segment pair to the next, except when the tip pair is reached.

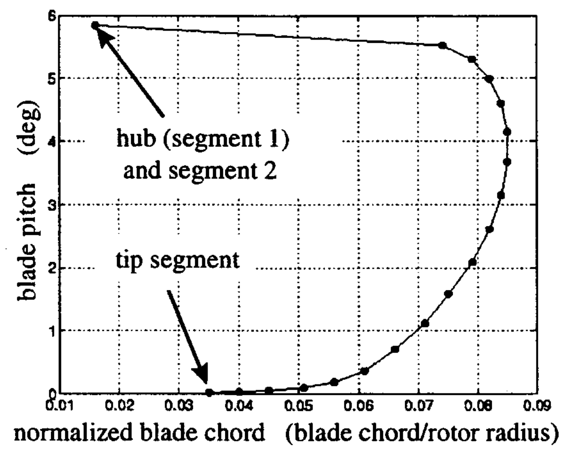

Figure A- 1. AWT-26 Blade Twist Data

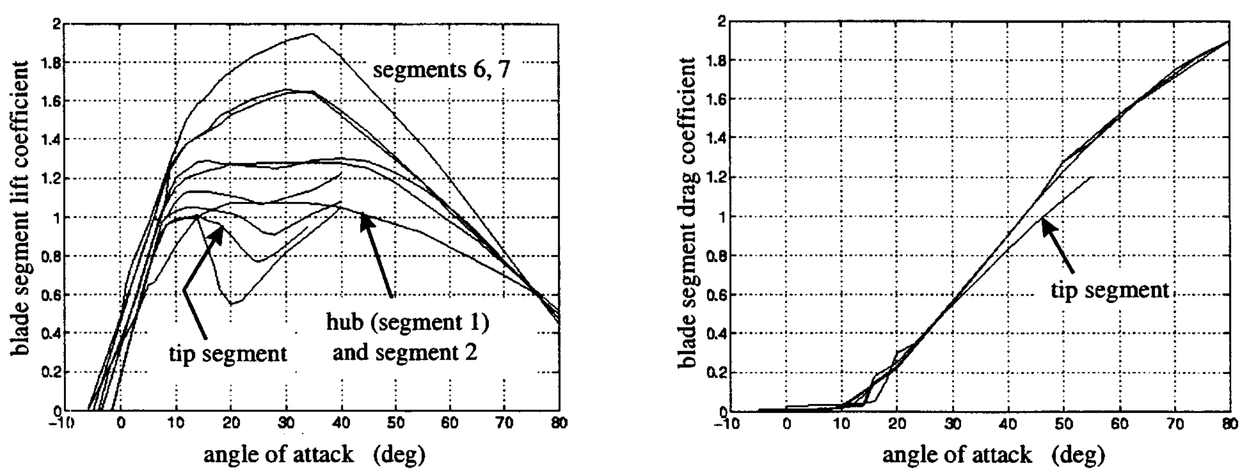

Figure A- 2. AWT-26 Blade Aerodynamic Data